PROCEEDINGS OF SPIE

Fiber Lasers VII: Technology, Systems, and Applications

Kanishka Tankala
Jay W. Dawson
Editor

25–28 January 2010
San Francisco, California, United States

Sponsored by
SPIE

Cosponsored by
Fianium Ltd. (United Kingdom)
PolarOnyx, Inc. (United States)

Published by
SPIE

Volume 7580

Proceedings of SPIE, 0277-786X, v. 7580

The papers included in this volume were part of the technical conference cited on the cover and title page. Papers were selected and subject to review by the editors and conference program committee. Some conference presentations may not be available for publication. The papers published in these proceedings reflect the work and thoughts of the authors and are published herein as submitted. The publisher is not responsible for the validity of the information or for any outcomes resulting from reliance thereon.

Please use the following format to cite material from this book:
Author(s), "Title of Paper," in *Fiber Lasers VII: Technology, Systems, and Applications*, edited by Kanishka Tankala, Jay W. Dawson, Proceedings of SPIE Vol. 7580 (SPIE, Bellingham, WA, 2010) Article CID Number.

ISSN 0277-786X
ISBN 9780819479761

Published by
SPIE
P.O. Box 10, Bellingham, Washington 98227-0010 USA
Telephone +1 360 676 3290 (Pacific Time) · Fax +1 360 647 1445
SPIE.org

Printed in the United States of America.

Publication of record for individual papers is online in the SPIE Digital Library.

SPIE Digital Library

SPIEDigitalLibrary.org

Paper Numbering: Proceedings of SPIE follow an e-First publication model, with papers published first online and then in print and on CD-ROM. Papers are published as they are submitted and meet publication criteria. A unique, consistent, permanent citation identifier (CID) number is assigned to each article at the time of the first publication. Utilization of CIDs allows articles to be fully citable as soon they are published online, and connects the same identifier to all online, print, and electronic versions of the publication. SPIE uses a six-digit CID article numbering system in which:

- The first four digits correspond to the SPIE volume number.
- The last two digits indicate publication order within the volume using a Base 36 numbering system employing both numerals and letters. These two-number sets start with 00, 01, 02, 03, 04, 05, 06, 07, 08, 09, 0A, 0B … 0Z, followed by 10-1Z, 20-2Z, etc.

The CID number appears on each page of the manuscript. The complete citation is used on the first page, and an abbreviated version on subsequent pages. Numbers in the index correspond to the last two digits of the six-digit CID number.

Contents

ULTRAFAST SOURCES

FIBER DESIGNS AND FABRICATION I

HIGH POWER SOURCES

BEAM COMBINING I

BEAM COMBINING II

POSTER SESSION

Conference Committee

Symposium Chairs

Donald J. Harter, IMRA America, Inc. (United States)
Peter R. Herman, University of Toronto (Canada)

Symposium Cochairs

Alberto Piqué, Naval Research Laboratory (United States)
Friedhelm Dorsch, TRUMPF Photonics (United States)

Program Track Chair

Gregory J. Quarles, VLOC (United States)

Conference Chair

Kanishka Tankala, Nufern (United States)

Cochair

Jay W. Dawson, Lawrence Livermore National Laboratory (United States)

Program Committee

Jes Broeng, Crystal Fibre A/S (Denmark)
Fabio Di Teodoro, Northrop Grumman Space Technology (United States)
Mark Dubinskii, Army Research Laboratory (United States)
Benjamin J. Eggleton, The University of Sydney (Australia)
Jean-Philippe Fève, Directed Energy Solutions (United States)
Almantas Galvanauskas, University of Michigan (United States)
Denis V. Gapontsev, Consultant (Russian Federation)
Anatoly B. Grudinin, Fianium Ltd. (United Kingdom)
Clifford Headley III, OFS Laboratories (United States)
Eric C. Honea, Lockheed Martin Aculight (United States)
Yoonchan Jeong, University of Southampton (United Kingdom)
Dahv A. V. Kliner, JDSU (United States)
Oliver Schmidt, Friedrich-Schiller-Universität Jena (Germany)
L. Brandon Shaw, Naval Research Laboratory (United States)
Thomas M. Shay, Air Force Research Laboratory (United States)
James Roy Taylor, Imperial College London (United Kingdom)
William E. Torruellas, The Johns Hopkins University Applied Physics Laboratory (United States)

Andreas Tünnermann, Fraunhofer-Institut für Angewandte Optik und Feinmechanik (Germany)
Robert G. Waarts, nLIGHT Corporation (United States)
Ji Wang, Corning Inc. (United States)
Benjamin G. Ward, U.S. Air Force Academy (United States)
Frank W. Wise, Cornell University (United States)

Session Chairs

1 Pulsed Sources
Robert G. Waarts, Robert Waarts Consulting (United States)

2 Materials Properties and Photodarkening
Yoonchan Jeong, University of Southampton (United Kingdom)

3 Mid-IR Sources and Frequency Conversion
Fabio Di Teodoro, Northrop Grumman Aerospace Systems (United States)

4 Visible and UV Lasers: Joint Session with Conferences 7578 and 7582
Dahv A. V. Kliner, JDSU (United States)
Peter E. Powers, University of Dayton (United States)
Norman Hodgson, Coherent, Inc. (United States)

5 Fiber Laser Market
Jes Broeng, NKT Photonics A/S (Denmark)

6 Applications I
William E. Torruellas, The Johns Hopkins University (United States)

7 Applications II
Anatoly B. Grudinin, Fianium Ltd. (United Kingdom)

8 Ultrafast Sources
Almantas Galvanauskas, University of Michigan (United States)

9 Fiber Designs and Fabrication I
Ji Wang, Corning Inc. (United States)

10 Fiber Designs and Fabrication II
Jeus Limpert, Friedrich-Schiller-Universität Jena (Germany)

11 Components
Benjamin G. Ward, U.S. Air Force Academy (United States)

12 Narrow Linewidth Sources and SBS Suppression
Mark Dubinskii, Army Research Laboratory (United States)

13 High Power Sources
Denis V. Gapontsev, Consultant (Russian Federation)

14 Beam Combining I
Eric C. Honea, Lockheed Martin Aculight (United States)

15 Beam Combining II
L. Brandon Shaw, U.S. Naval Research Laboratory (United States)

16 Late-Breaking News
Jay W. Dawson, Lawrence Livermore National Laboratory (United States)

Best Student Oral Presentation Award Ceremony and Vote of Thanks
Kanishka Tankala, Nufern (United States)
Jay W. Dawson, Lawrence Livermore National Laboratory (United States)

Multi-Colour Vortex Beam Generation by Cascaded Raman Processes in Optical Fibers

Siddharth Ramachandran[1*], Christian Smith[2], Peter Balling[2], Poul Kristensen[3]

[1]*Department of Electrical & Computer Engineering and Photonics Center, Boston University, Boston, MA, USA*
[2]*Department of Physics and Astronomy, Aarhus University, Aarhus, Denmark*
[3]*OFS-Fitel ApS, Broendby, Denmark*

**sidr@bu.edu*

***Abstract**: We exploit stimulated-Raman-scattering to generate polarisation-vortices over 4 Stokes shifts (53 THz) with a specially-designed optical fiber. This illustrates the possibility of generating these beams, of immense recent interest, at any wavelength that nonlinear processes in glass allow.*

Polarisation vortex beams (especially radially polarised light – see pattern in Fig. 1a) have recently attracted immense interest due to characteristics such as enhanced laser-machining efficiencies[1], resistance to turbulence in free-space propagation[2], and higher resolution for microscopy[3], to name a few. Given the variety of applications, it would be desirable to have the means of generating them at the wavelength and power of choice. Current generation techniques primarily rely on a conventional laser beam converted into a vortex beam by means of a free-space component[4,5], which limits the power or wavelengths at which they can be realised. In this paper, we demonstrate the possibility of generating vortex beams at a variety of desired colours by exploiting cascaded Raman scattering in a fiber that stably supports these beams. To the best of our knowledge, this represents the first demonstration of any nonlinear-optical interaction with polarisation vortex beams.

The key enabler for our experiments is a specially designed fiber that allows signal propagation in vortex modes over lengths as large as 100 m – in contrast, previous attempts at generating these modes in fibers could not achieve more than a few cm of propagation in a fiber held rigidly straight[6]. Since this fiber allows long-distance propagation of a vortex beam, well-known fiber-nonlinear processes can then be used to manipulate them. In this paper, we exploit stimulated Raman scattering (SRS) to obtain radially polarised beams with high powers (P_{peak} up to 470 W) and at a variety of wavelengths as far apart as 240 nm (53 THz) from the pump wavelength. This represents a shift of up to the 4th Stokes order of a 1064-nm pulsed pump source.

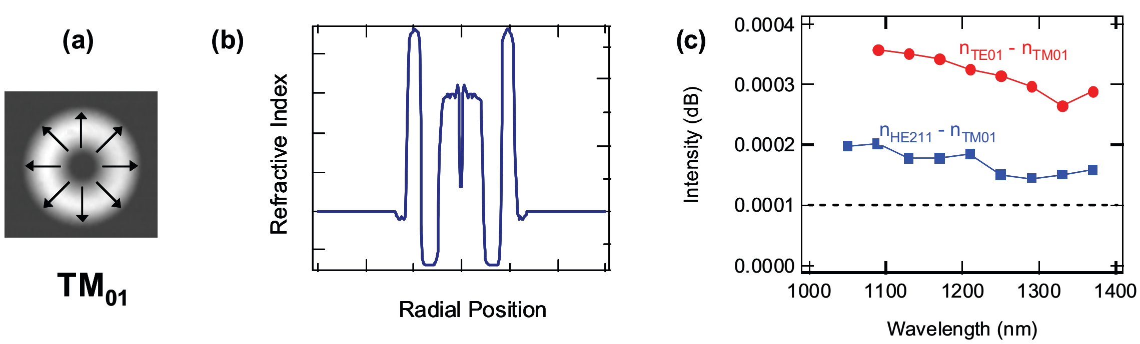

Fig. 1: (a) Mode intensity image of a radially polarised beam; (b) Annular refractive index profile of specialty fiber that breaks the degeneracy of vortex modes, (c) n_{eff} difference between desired radially polarised (TM_{01}) mode and other vortex modes as a function of wavelength.

The annular refractive index profile of this fiber, shown in Fig. 1b, enables stable, mode-coupling-free transmission of a selected polarisation vortex. This is because this design breaks the near-degeneracy of vortex modes (TM_{01}, TE_{01} and HE_{21}) in a conventional fiber, where the modes are usually separated in effective indices (n_{eff}) by ~10^{-6}. In contrast, Fig. 1c shows that the n_{eff} of the desired radially polarised mode (TM_{01}) is separated from the other states by more than 10^{-4}. Note that this index separation is similar to that of PM fibers – hence we conclude that, once excited, this mode will propagate stably over long lengths (we observed no degradation of mode quality after even 100-m propagation). The other important feature of this fiber is that this enhanced mode separation is maintained over several 100 nm, which suggests that any nonlinear-optical transformation of light in this mode will not diminish its inherent stability.

Details of the measurement setup are shown in Fig. 2a. A Nd:YAG laser (~10-ns Q-switched pulses at 1064 nm with 10 Hz rep. rate) serves as the input to the vortex fiber. A microbend-induced fiber grating (period ~ 500 µm) is used to convert the conventional input into a radially polarised beam. We independently measure that the conversion efficiency of this process is as high as ~99% at the input wavelength of 1064 nm. After 100-m fiber-propagation of the vortex mode, the output is collimated, and either sent directly to an OSA or power-meter, or wavelength separated, using bandpass filters at the fundamental (1064 nm), first (1115 nm) or second (1175 nm) Stokes shift, and then sent to a Si CCD camera to record images at different wavelengths. Fig. 2b shows the spectra of light from the output of the vortex fiber at various output power levels (labelled with both pulse energy and peak power). At the maximum energy level currently employed (4.7 µJ), we see up to the 4th order Stokes emission, roughly 240 nm away from the pump wavelength (53 THz shift). The insets in the plot of Fig. 2b show pure, doughnut-shaped mode images at the pump wavelength and all Stokes orders for a pump energy of 3.6 µJ. Thus, this confirms the central objective of these experiments – of nonlinear frequency generation *in* the desired mode as opposed to some random collection of multiple modes.

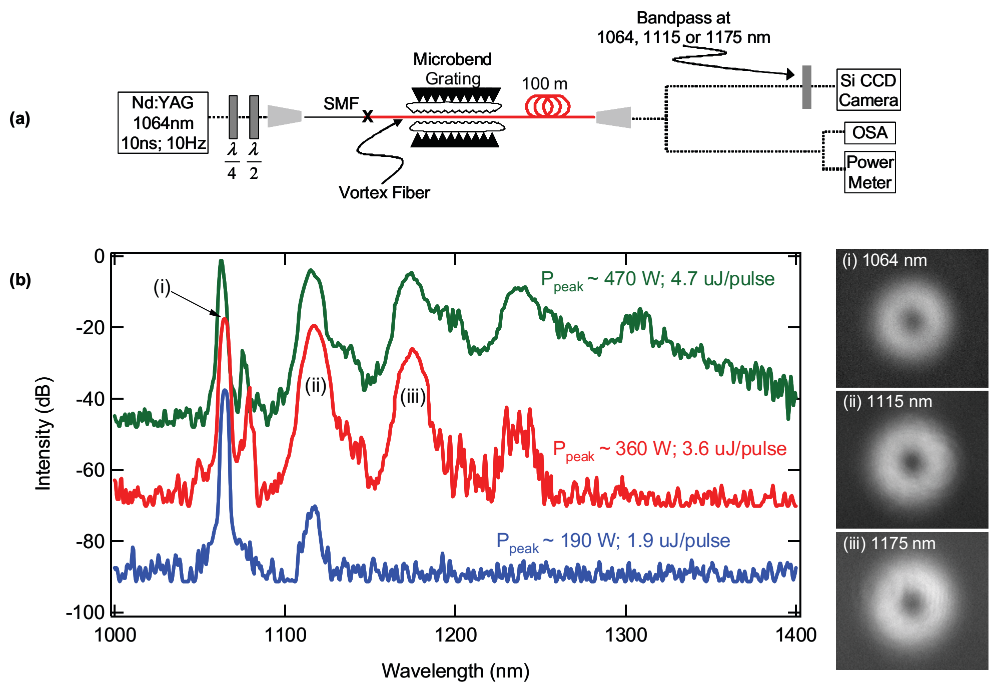

Fig. 2: (a) Schematic of experimental setup. Microbend grating creates polarisation vortex at pump wavelength (1064nm), which is then propagated through 100-m of fiber to observe nonlinear frequency generation through stimulated Raman scattering; (b) Output spectra for different pump (1064-nm light) powers, and mode images at the fundamental (i – 1064nm), 1st stokes shift (ii – 1115 nm) and 2nd stokes shift (iii – 1175 nm) at P_{pump} ~ 3.6 µJ confirming Raman shifting *in* the desired polarisation vortex.

In summary, we demonstrate nonlinear frequency generation of optical vortices (specifically polarisation vortices) via SRS in optical fibers. This provides crucial confirmation of the fact that a fiber that can stably propagate an optical vortex in the linear regime can also preserve its polarisation symmetry through nonlinear optical transformations. We show that powers as high as 470 W can be transmitted in polarisation vortex beams, and Raman stokes shifts up to 4th order were obtained. From a practical standpoint, this opens the door to generating optical vortices at a wide variety of wavelengths and over wide bandwidths, since fiber nonlinearities combined with dispersion control are especially versatile in this regard. This, in turn, promises to open new applications for these beams in areas that may need non-standard wavelengths and/or ultra-short pulses with wide bandwidths.

[1] A. V. Nesterov and V. G. Niziev, "Laser beams with axially symmetric polarization," *Journal of Physics D* **33**, 1817, 2000
[2] W. Cheng et al, "Propagation of vector vortex beams through a turbulent atmosphere," *Optics Express*, **17**, p. 17829, 2009
[3] R. Dorn et al, "Shaper focus for a radially polarized light beam," *Physical Review Letters* **91**, 233901, 2003
[4] G. Machavariani et al, "Efficient extracavity generation of radially and azimuthally polarized beams," *Optics Letters* **32**, 1468, 2007
[5] M.A. Ahmed et al, "Radially polarized 3 kW beam from a CO_2 laser with a intracavity resonant grating mirror," *Optics Letters* **32**, 1824, 2007
[6] S. Ramachandran et al, "Generation and propagation of radially polarized beams in optical fibers," *Optics Letters* **16**, 2525, 2009

Mid-IR laser emission from a C_2H_2 gas filled Hollow Core Photonic Crystal Fiber

Vasudevan Nampoothiri[1], Andrew M. Jones[2], Amarin Ratanavis[1], Rajesh Kadel[2], Natalie Wheeler[3],François Couny[3], Fetah Benabid[3], Brian R. Washburn[2], Kristan L. Corwin[2], and Wolfgang Rudolph[1]

[1]*Department of Physics, University of New Mexico, Albuquerque, NM 87131, USA*
[2]*Department of Physics, Kansas State University, Manhattan, KS 66506, USA*
[3]*Centre for Photonics and Photonics Materials, Department of Physics, University of Bath, BA2, 7AY, UK*
avvn@unm.edu, wrudolph@unm.edu

ABSTRACT: Lasing from population inversion in the mid-IR (3.1-3.2 μm) region was observed from a gas (acetylene) filled hollow core photonic crystal fiber when optically pumped at $\lambda \sim 1.5$ μm.
Key words: Molecular gas lasers, Fiber Lasers, Photonic crystal fibers

1. INTRODUCTION

Hollow core photonic crystal fibers (HC-PCF) have gained wide attention due to its ability to guide light in the hollow core with low attenuation over very long distances[1]. Many nonlinear optical phenomena, including the demonstration of a Raman laser[2] has been observed in gas filled photonic crystal fibers. Here we report what we believe is the first demonstration of an optically pumped gas laser (OPGL) based on population inversion in a hollow core photonic crystal fiber (HC-PCF). With large possible stokes shift compared to atomic vapor lasers, OPGLs with molecular gases are attractive candidates for generating coherent radiation in the mid-infrared. In our experiment, we optically pump acetylene (C_2H_2) filled Kagome structured hollow core fiber with 1.5 μm nanosecond pulses from an optical parametric oscillator (OPO). Kagome fiber exhibits strong guiding in the near IR pump region (loss < 0.75 dB/m) and weak guiding behavior at about 3 μm (~20 dB/m), as calculations suggest. We observe laser emission in the mid-IR region at wavelengths of 3.12 μm and 3.16 μm. The laser combines the advantages of fiber lasers, such as the confinement of pump and laser light over long interaction lengths in a compact configuration, with those of gas lasers: high damage thresholds, a wide variety of possible (eye-safe) emission wavelengths in the atmospheric transmission window and the potential for coherent emission from mutually incoherent pump sources. The feasibility of implementing molecular OPGLs inside a waveguide has been previously examined[3].

2. SETUP FOR THE OPGL INSIDE HC-PCF

In this initial demonstration of a fiber OPGL, ns pulses excite acetylene gas inside HC-PCF. This approach is motivated by an OPGL based on acetylene vapor inside a gas cell that demonstrated large optical gain near 3 μm[4]. The layout of the optically pumped hollow core fiber gas laser is shown in Fig.1 (a).

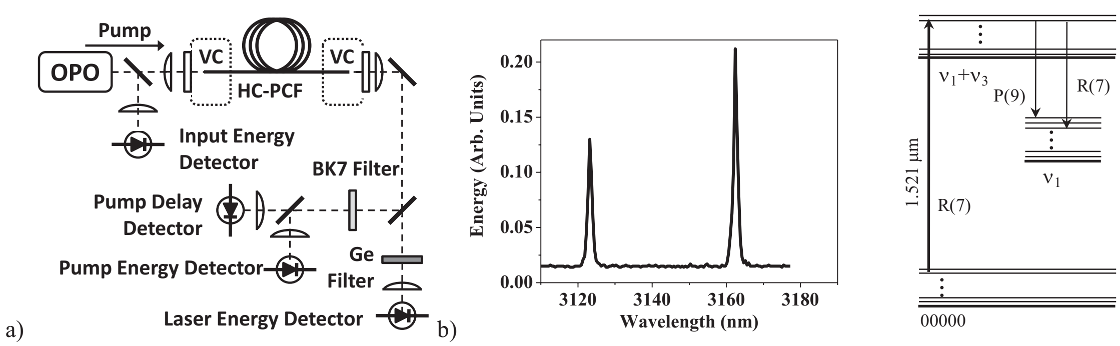

Fig. 1: a) Fiber OPGL setup. The acetylene filled HC-PCF is pumped using a nanosecond OPO. Suitable filters were used to separate laser emission from pump. b) Spectrum of laser output when C_2H_2 pressure was ~7 torr and a simplified energy level diagram of C_2H_2 showing the pump and two laser transitions.

A 1.65-m single-cell Kagome structured hollow core fiber was filled with C_2H_2 in a vacuum chamber. An optical parametric oscillator is used as the pulsed pump source, and its output pulses were typically 5 – 6 ns in duration with average pulse energies of ~ 5 mJ. The OPO was tuned to resonance with the $\nu_1 + \nu_3$ (R7) transition in $^{12}C_2H_2$ at λ = 1521.06 nm. The gain of the laser is sufficient that no cavity was required, in spite of the large loss in the lasing band.

3. CHARACTERIZATION OF THE LASER OUTPUT

Spectral output from the OPGL is shown in Fig. 1b for ~ 7 torr acetylene gas pressures. The laser emission shows two peaks at 3.12 μm and 3.16 μm. The OPO pump, tuned to the R(7) rotational transition, moves population from the J = 7 rotational state of the ground state vibrational manifold to the J = 8 rotational state of the $\nu_1 + \nu_3$ vibrational state creating a population inversion between J = 8, $\nu_1 + \nu_3$ state and the essentially empty ν_1 vibrational state. This result in the lasing transition from the J = 8, $\nu_1 + \nu_3$ state to the allowed rotational states of ν_1 vibrational state. Using the known molecular constants for the ν_1 and $\nu_1 + \nu_3$ states[5], the two peaks are identified as the R(7) and P(9) transitions originating from pump level of the $\nu_1 + \nu_3$ vibrational state and terminate at the J = 7 and J = 9 of the ν_1 vibrational state. Pulsed laser output was observed for gas pressures between 0.5 torr and 20 torr.

Figure 2(a) shows the laser pulse energy output as a function of pump pulse energy for an acetylene pressure of 7 torr. This curve indicates the onset of saturation as the increasing pump pulse energy starts to saturate the absorption transition. At lower pressures, saturation is more pronounced. Figure 2(b) shows the lasing output as a function of acetylene pressure for pump energies of 600 nJ coupled into the fiber (30 μJ incident on the fiber). The coupling efficiency was only ~2%, but values exceeding 50% into Kagome fiber have been demonstrated. The measured temporal delay between the pump and laser pulses showed shorter delays when the pump power is further above threshold when population inversion builds up more quickly. The lasing threshold, defined as the minimum pump pulse energy coupled into the fiber necessary to observe mid-IR laser output, is about 200 nJ, and varies with pressure. The slope efficiency of the laser, defined as the change in output energy divided by the change in pump energy coupled into the fiber, is a few percent.

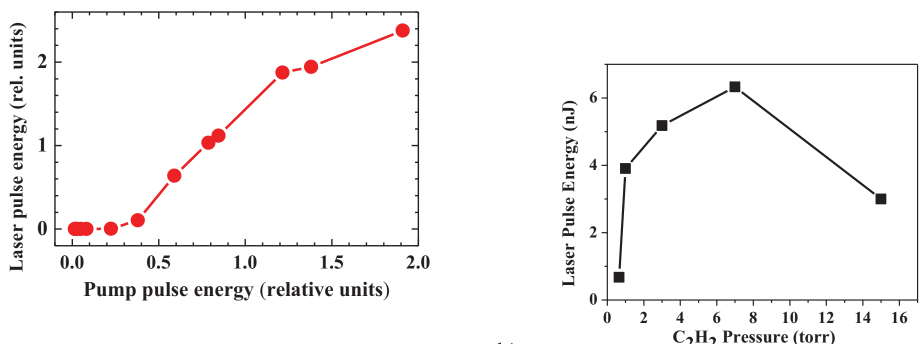

a) b)

Fig. 2: a) Laser pulse output energy vs. pump pulse energy in relative units, for 7 torr pressure acetylene gas. b) Mid-IR laser output power vs. acetylene pressure when pumped at 30 μJ incident input pulse energy for several acetylene pressures inside the HC-PCF.

The reduction of the Kagome fiber losses at the laser wavelength should substantially increase the slope efficiency and decrease the threshold. Furthermore, the addition of an optical cavity or increased Kagome fiber length may also improve laser performance. While this first demonstration uses a pulsed pump, the gas-filled fiber laser is particularly attractive for pumping with continuous wave laser sources.

4. ACKNOWLEDGEMENTS

This work was supported by the Air Force Office of Scientific Research (FA9550-08-1-0344), Army Research Office (W911NF-08-C-0106 and W911NF-08-1-0332), National Science Foundation (PHY-0722622), Joint Technology Office (W911NF-05-1-0507), Engineering and Physical Sciences Research Council, and Precision Photonics Corp.

5. REFERENCES

[1] P. J. Roberts, F. Couny, H. Sabert, B. J. Mangan, D. P. Williams, L. Farr, M. W. Mason ,A. Tomlinson, T. A. Birks, J. C. Knight, and P. St.J. Russell, "Ultimate low loss of hollow-core photonic crystal fibres", Optics Express **13** (2005) 236-244.

[2] F. Couny, F. Benabid, and P. S. Light, "Subwatt Threshold cw Raman Fiber-Gas Laser Based on H_2-Filled Hollow-Core Photonic Crystal Fiber", Physical Review Letters **99**, (2007) 143903-1—143903-4.

[3] A. Ratanavis, N. Campbell, A. V. V. Nampoothiri, and W. Rudolph, "Performance and Spectral Tuning of Optically Overtone Pumped Molecular Lasers", *IEEE J of Quantum Electronics,* **45** (2009) 488-498.

[4] A.V.V. Nampoothiri, A Ratanavis, N. Campbell, and W. Rudolph, "Molecular C_2H_2 and HCN lasers pumped by an optical parametric oscillator in the 1.5-μm band", submitted to Optics Express, 2009.

[5] M.Herman, A.Campargue, M. I. El Idrissi, and J. Vander Auwera, "Vibrational Spectroscopic Database on Acetylene, $X^1\Sigma_g^+$ ($^{12}C_2H_2$, $^{12}C_2D_2$, and $^{13}C_2H_2$)", J. Phys. Chem. Ref. Data **32,** 921-1361 (2003).

Coherent Combination of a 1.26-kW Fiber Amplifier

S. J. McNaught, G. D. Goodno, P. A. Thielen, M. G. Wickham, M. E. Weber, and J. E. Rothenberg*
*Northrop Grumman Aerospace Systems, R1-2194B, One Space Park, Redondo Beach, CA 90278, * josh.rothenberg@ngc.com*

Abstract: A 1.26-kW, multi-stage Yb fiber MOPA was coherently combined using active polarization and phase control with 94% visibility to a second fiber amplifier, consistent with estimated decoherence effects from fiber nonlinearity, linewidth, and phasing accuracy.

1. Introduction: Actively phase-locked coherent beam combining (CBC) of high power lasers provides a method for parallel scaling of laser brightness past the limits of any single laser element [1]. In this method, a master oscillator (MO) seeds an array of power amplifiers (PAs) whose outputs are locked in phase using active feedback and combined to form a single high-brightness beam. This MOPA architecture was employed to combine seven Nd:YAG slab amplifier chains into a composite 105 kW [2]. While this represents a significant achievement in laser power scaling, a CBC array of Yb-doped fiber amplifiers (YDFAs) offers potential for improved performance.

The primary concern for CBC with high power YDFAs is preserving the coherence properties of the MO to allow fully constructive interference of the amplified outputs. High power, single mode (SM) fiber lasers exhibit significant nonlinear responses. While 10 kW output has been demonstrated from a near-SM fiber [3], its spectrum spans tens of nm owing to nonlinear broadening, preventing its use as an amplifier in a CBC array. Actively phase-locked CBC of fiber lasers is implemented either with a single-frequency (SF) MO, which has been limited to ~150 W per fiber due to stimulated Brillouin scattering (SBS), or with controlled linewidth broadening to suppress SBS [4]. 10-GHz class, linewidth-broadened SM YDFAs have recently been demonstrated at kW-class powers [5,6].

In this work, we integrated a phase-modulated 21-GHz linewidth, 1.26-kW YDFA chain with active phase and polarization control to demonstrate combining with over 94% mutual coherence to a second, parallel fiber amplifier. This represents an increase of nearly an order of magnitude in power for active phase-locking of a fiber amplifier over previously reported work [4] and shows that decoherence effects from active phase control, fiber nonlinearities, and coherence length are manageable at these power levels.

2. Experimental Configuration: A schematic of the combining experiment is shown in Fig 1. A SF fiber MO (NP Photonics) operating at a wavelength λ = 1064 nm is phase-modulated using a waveguide electro-optic modulator (EOM) to 21 GHz FWHM linewidth for SBS suppression. Following the EOM, the output is amplified to ~100 mW and split into three channels, one of which is frequency-shifted by a 55-MHz acousto-optic modulator to serve as a heterodyne reference for phase metrology. Each of the other two channels contains an EOM for piston phase control, a variable delay line (VDL) for path equalization, and gain-staged YDFAs. The low power channel contains two polarization-maintaining (PM) pre-amplifiers to provide ~1 W output power. The high power channel contains a 12-dB PER fiber polarization controller (General Photonics, POS-104) followed by a recently developed 3-stage, non-PM YDFA chain (IPG Photonics) to boost power to 1.26 kW. The final power amplifier of this YDFA is pumped by 1018 nm fiber lasers and has been described in [6]. The amplified spectrum is identical to the seed.

Fig. 1. Schematic of fiber CBC experiment. Fringe visibility of the combined outputs indicates mutual coherence and combining efficiency.

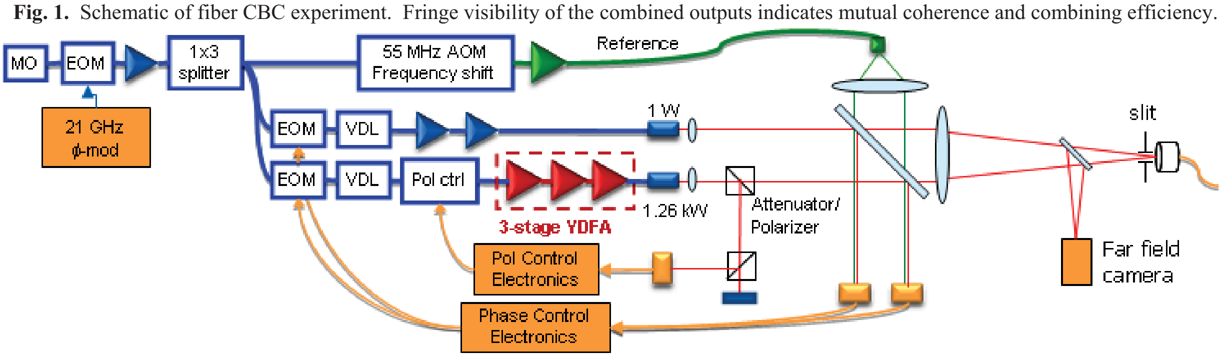

The outputs from both fiber amplifier channels are collimated and tiled side-by-side. The high power beam is attenuated for amplitude equalization with the low power beam and polarization-filtered to provide a feedback signal for the polarization controller. The frequency-shifted reference is combined with the 2x1 tiled beam. Separate photodetectors in each channel sense the phase of the 55-MHz beat notes to provide error signals for phase-locking of each beam to the reference with fidelity of $\lambda/80$ RMS [7]. Tolerance stack-up of uncorrelated errors means that the beam-to-beam phasing errors are $\Delta\phi = 2^{1/2}(\lambda/80) = 0.11$ rad. A low-power sample of the tiled beam is focused onto a far field camera to generate a stationary fringe pattern. A narrow slit whose width is ~5% of a fringe period provides a metric for mutual coherence between the two beams through the visibility $V = (I_{max} - I_{min})/(I_{max} + I_{min})$. I_{max} and I_{min} are, respectively, the transmitted intensities through the slit at a peak and a null of the far-field interference pattern, measured sequentially by applying a π–phase shift to the phase controller for one channel. With proper amplitude equalization between the two phase-locked channels, V is equivalent to the mutual coherence between the two beams and is representative of the coherent combining efficiency for co-aligned beams.

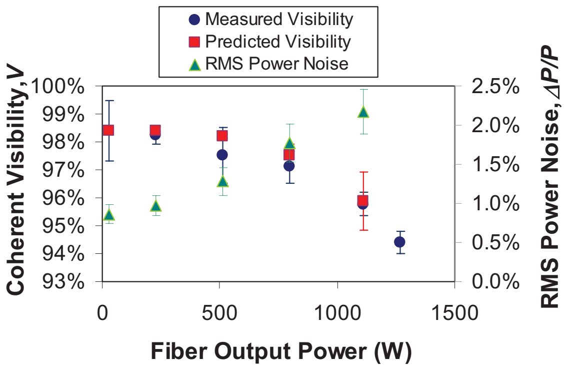

Fig. 2. Measured and predicted coherent visibility V due to self-phase modulation arising from output power fluctuations.

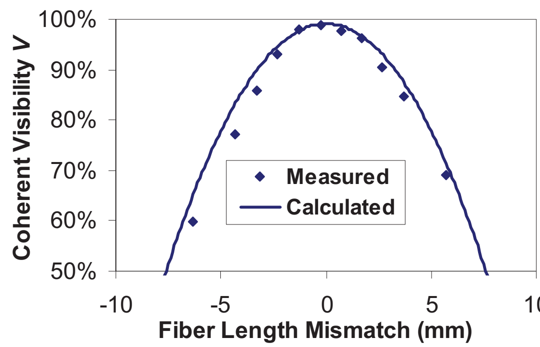

Fig. 3. Loss of visibility (decoherence) due to 21-GHz linewidth and path mismatch between fiber channels.

3. Results and discussion: Fig 2 shows the measured mutual coherence V of the combined phase-locked beam as a function of output power from the high power amplifier channel. Over 94% mutual coherence was measured at the full 1.26 kW output power. This measurement encompasses all physical decoherence effects that could limit combining efficiency, including path mismatch, beam jitter, mode dynamics, amplitude noise, nonlinear phase shifts or spectral distortion, amplified stimulated emission (ASE), and SBS. The low power coherence agrees with the expected limit based on the accuracy of active phase control [8], $1 - \Delta\phi^2 = 1 - (0.11 \text{ rad})^2 = 0.988$.

Much of the coherence drop with increasing power can be attributed to power-dependent nonlinear phase noise $\Delta\phi_{NL}$ arising from self-phase modulation (SPM) in the fiber [9]. Fluctuations ΔP in amplified output power P induce a nonlinear phase shift $\Delta\phi_{NL} = (\mathrm{d}\phi_{NL}/\mathrm{d}P)\Delta P$, where $\mathrm{d}\phi_{NL}/\mathrm{d}P = 2\pi n_2(L_{eff}/A_{eff})/\lambda$, L_{eff} and A_{eff} are the effective power-weighted fiber length and mode field area, respectively, and n_2 is the nonlinear index for silica fiber. Any RMS power noise ΔP faster than the ~10 kHz closed loop phase control bandwidth [7] will result in SPM that will be uncorrected and will contribute to decoherence and a drop in V: $V(\Delta P) = V(0)[1 - (\mathrm{d}\phi_{NL}/\mathrm{d}P)^2 \cdot \Delta P^2/2]$. The differential shift was measured $\mathrm{d}\phi_{NL}/\mathrm{d}P = (1.07 \pm 0.15 \text{ rad})/(114 \pm 10 \text{ W}) = 9.4 \pm 1.7$ rad/kW. Based on measured power fluctuations $\Delta P/P$, the predicted values agree with the observed decoherence up to 1.1 kW (Fig 2).

Owing to the relatively broad 21-GHz linewidth, optical path lengths in each YDFA must be equalized to within a small fraction of the coherence length to prevent significant combining loss due to decoherence [9]. Fig 3 shows the measured drop in V as the path length is adjusted, and agrees with the calculated coherence function. A key question for practical operation of a large array of kW-class fibers is whether the change in fiber path due to thermal expansion and index changes upon turn-on will result in significant decoherence. The measured path change at 1.26 kW is ~1.5 mm, suggesting combining losses owing to coherence length issues can be kept below 1% with modest attention to amplifier thermal responses.

4. Conclusions and future directions: The demonstration of >94% visibility coherent combination of a 21-GHz, 1.26-kW YDFA opens the door to integration of such fibers in large CBC arrays. There appears to be room for further YDFA power scaling by changing the pumping scheme from 1018-nm fibers to 980-nm diodes [5,6], which should enable shortening the fiber length and reducing the fiber nonlinearity. Implementation of active path length controls seems likely to enable CBC of fibers with linewidths substantially broader than 21 GHz.

[1] T.Y. Fan, IEEE J. Sel. Topics Quantum Elect. **11**, 567 (2005).
[2] S. McNaught et al, Conference on Lasers and Electro-Optics (CLEO), paper CThA1 (2009).
[3] V. Gapontsev, V. Fomin, and A. Yusim, Solid State and Diode Laser Technology Review, Newton, MA (2009).
[4] J. Anderegg et al, "Coherently coupled high-power fiber arrays," Proc. SPIE **6102**, p. 61020U1 (2006).
[5] J. Edgecumbe et al, 11th Annual Directed Energy Symposium, Honolulu, HI (2008).
[6] O. Shkurikhin, V. Gapontsev, and N. Platonov, SSDLTR, Newton, MA (2009).
[7] G. D. Goodno et al, IEEE J. Selected Topics in Quantum Elect. **13**, 460 (2007).
[8] C. D. Nabors, "Effect of phase errors on coherent emitter arrays," Appl. Opt., **33**, 2284 (1994).
[9] G. D. Goodno and J. E. Rothenberg, OSA Annual Meeting, paper FTuW1 (2008).

1-kW, All-Glass Tm:fiber Laser

Thomas Ehrenreich, Ryan Leveille, Imtiaz Majid, and Kanishka Tankala
Nufern, Inc. (United States)

Glen Rines and Peter Moulton
Q-Peak, Inc. (United States)

The Tm:fiber laser is a promising source of high-power, eyesafer, 2000-nm power. Starting in 1998, the power output and efficiency of double-clad, Tm-doped fibers have both steadily risen. In published work, we have previously reported a total of 885 W of multimode power from two ends of a free-space-pumped, multimode Tm:silica fiber laser, with 50% optical-optical efficiency. Northrop Grumman, also using free-space pumping, has reported 608 W of single-mode, single-frequency power.

While free-space pumping provides a convenient scheme for scaling studies, the need to maintain a critical mechanical alignment of the pump power into the cladding limits use outside of a laboratory environment. In terms of all-glass Tm:fiber systems, where the pump light is delivered to the cladding through all-fiber-based couplers, the highest reported power until now was 415 W, in an IPG fiber-laser-pumped system with Yb,Er:fiber pump sources.

Here we report a >1 kW, all-glass, Tm:silica fiber laser MOPA system, with the amplifier pumped by twelve, fiber-coupled 792-nm diode sources. In initial work with the all-glass design, we obtained 503 W at 2045 nm, with a 50-W oscillator and a co-pumped amplifier consisting of 10 m of 20 (0.1 NA)/400 (0.46 NA) μm double-clad fiber driven by six diode pumps connected to a 6+1:1 pump coupler. The amplifier optical slope efficiency was 61%. To scale to higher powers, we lengthened the active fiber to 12 m, added a cladding stripper, another co-pumping coupler and 12 m of 20/400 active fiber to output end of the first amplifier fiber. With the added power of six more pump diodes, we obtained 1053 W of power, with an overall optical slope efficiency of 53%. Given past results with the same fiber, we expect the output to be single mode, and we are in the process of verifying this at the full power level.

Compact all-fiber optical Faraday isolator

L. Sun,*[a,b] S. Jiang,[c] and J. R. Marciante[a,b]
[a]Laboratory for Laser Energetics, University of Rochester, Rochester, NY 14623;
[b]Institute of Optics, University of Rochester, Rochester, NY 14627, USA
[c]AdValue Photonics Inc, 4585 S. Palo Verde Road, Suite 405, Tucson, AZ 85714, USA

ABSTRACT

An all-fiber optical Faraday isolator is demonstrated. It consists of two fiber polarizers and a fiber Faraday rotator, which is made of a 4-cm-long, 65-wt%-terbium–doped silicate fiber. The effective Verdet constant of the terbium-doped fiber was measured to be 32.1±0.8 rad/(Tm), which is 27× larger than that of silica fiber. This effective Verdet constant is 83% of the Verdet constant of commercially available crystal (TGG) used in bulk optics–based isolators and 61% larger than previously reported values. The fiber polarizers are Helica-in-Fiber Polarizers (Chiral Photonics). The isolation of this fully fusion spliced all-fiber isolator is measured to be 19 dB.

Keywords: Faraday isolator, terbium-doped fiber, effective Verdet constant

1. INTRODUCTION

Optical isolators are important components in optical communication networks and laser systems. Although all-fiber optical isolators are preferred for high-power applications, current isolators are based on bulk optics. The small Verdet constant [~1.1 rad/(Tm) at 1060 nm] of silica fiber is the bottleneck to realizing all-fiber Faraday isolators. In this paper, we report on the demonstration of a compact all-fiber Faraday isolator.

2. TERBIUM-DOPED FIBER

Terbium doping is an effective way to increase the Verdet constant in a fiber. Highly terbium doped silicate glasses have been designed and fabricated. Boron oxide and aluminum oxide were added into the glass composition to improve the solubility of terbium oxide. A 65-wt%-terbium-oxide–doped glass was used as the core glass. The rod-in-tube technique was used for single-mode fiber fabrication. The fiber-pulling temperature was around 1000°C. The numerical aperture and diameter of the core were 0.083 and 7.4 μm, respectively, and the cladding diameter of the fiber was 125 μm. The propagation loss of the fiber was measured to be 0.024 dB/cm at 1310 nm using the cut-back technique. The fiber was fabricated at AdValue Photonics using an in-house fiber drawing tower.

Using the measurement technique described in Ref. 1, Fig. 1 shows the measured rotation angle and the corresponding curve fit at the 1053-nm measurement wavelength as the magnet was translated along the length of the fiber. The maximum rotation angle reached 45°C. The error in the measured angle was primarily caused by air flow and it was determined to be 1° by a polarization-stability measurement. The effective Verdet constant was determined to be –32.1±0.8 rad/(Tm), which is 27× larger than that of silica fiber. This effective Verdet constant is 83% of the Verdet constant of commercially available crystal (TGG) used in bulk optics–based isolators and 61% larger than previously reported values.[2]

3. EXPERIMENT

The experimental configuration is shown in Fig. 2. A 4-cm section of Tb-doped fiber, spliced between two 15-cm sections of single-mode (SM) fiber, went through a magnet tube. The N48 NdFeB magnet tube (residual flux density B_r = 0.95 T) was 4 cm long with inner and outer diameters of 5 mm and 6 cm, respectively. The two other ends of the SM fibers were each spliced to a fiber polarizer. The fiber polarizers were Helica In-Fiber Polarizers (Chiral Photonics),[3] which consist of 4-cm-long chiral scattering grating (CSG) with polarization-maintaining (PM) fiber pigtails at both ends. The polarization directions of the two fiber polarizers were aligned with a rotational difference of 45°. The optical isolation at 1053 nm was measured to be 19 dB.

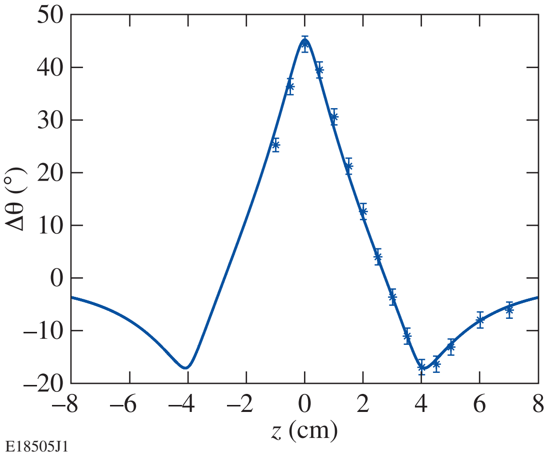

Figure 1. Measured rotation angle (stars) and corresponding curve fit (solid) at a 1053-nm wavelength as a function of the magnet's location along the fiber's *z* axis.

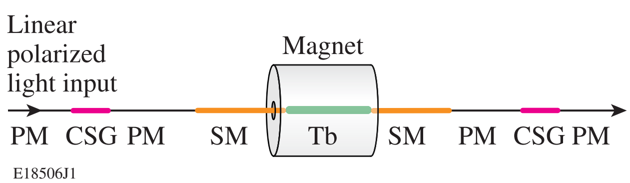

Figure 2. Experimental configuration of the all-fiber Faraday isolator.

4. CONCLUSION

In conclusion, an all-fiber optical Faraday isolator is demonstrated. It consists of two fiber polarizers and a fiber Faraday rotator, which is made of a 4-cm-long, 65-wt%-terbium–doped silicate fiber. The effective Verdet constant of the terbium-doped fiber was measured to be 32.1±0.8rad/(Tm), which is 27× larger than that of silica fiber. This effective Verdet constant is 83% of the Verdet constant of commercially available crystal (TGG) used in bulk optics–based isolators and 61% larger than previously reported values. The fiber polarizers are Helica In-Fiber Polarizers (Chiral Photonics). The isolation of this fully fusion-spliced all-fiber isolator was measured to be 19 dB.

ACKNOWLEDGMENT

This work was supported by the U.S. Department of Energy Office of Inertial Confinement Fusion under Cooperative Agreement No. DE-FC52-08NA28302, the University of Rochester, and the New York State Energy Research and Development Authority. The support of DOE does not constitute an endorsement by DOE of the views expressed in this article. This work is also supported in part by Wright-Patterson Air Force Research Laboratory (WPAFRL) under contract FA8650-09-C-5433. The authors would like to acknowledge the technical support of Dr. R. L. Nelson and W. D. Mitchell from WPAFRL.

REFERENCES

[1] L. Sun, S. Jiang, J. D. Zuegel, and J. R. Marciante, "Effective Verdet constant in a terbium-doped-core phosphate fiber," *Opt. Lett.* **34**(11), 1699–1701 (2009).

[2] J. Ballato and E. Snitzer, "Fabrication of fibers with high rare-earth concentrations for Faraday isolator applications," *Appl. Opt.* **34**(30), 6848–6854 (1995).

[3] V. I. Kopp, V. M. Churikov, and A. Z. Genack, "Synchronization of optical polarization conversion and scattering in chiral fibers," Opt. Lett. **31**, 571–573 (2006).